Published March 13, 2014

Original Research

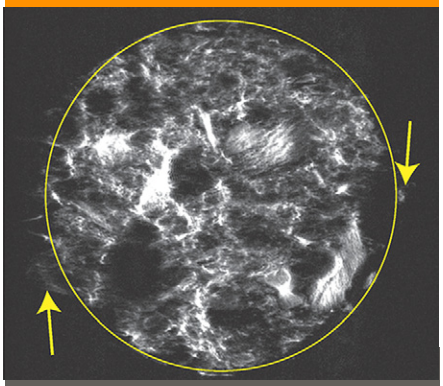

Magnetic resonance imaging is becoming an important tool in the agricultural sector. Diffusion tensor imaging (DTI), until recently mainly a neuroscience tool, was used to provide in situ three-dimensional images of plant roots grown in small pots. The DTI experiments were able to map roots and shoots.

In Situ Magnetic Resonance Imaging of Plant Roots

Marco L.H. Gruwel*

Visualization of the root system architecture of plants is possible using a combination of magnetic resonance imaging of water mobility and tractography. Diffusion tensor imaging (DTI), a magnetic resonance application, was used to provide a three-dimensional map of water mobility inside a pot containing soil and roots. Tractography generates channels that constitute pathways of facilitated water movement, representing the roots, calculated from water diffusion properties obtained from DTI experiments. Examples of pea (*Pisum sativum* L.) and corn [*Zea mays* L. var. *indentata* (Sturtev.) L.H. Bailey] root growth are provided.

Abbreviations: DTI, diffusion tensor imaging; FOV, field of view; MR, magnetic resonance; MRI, magnetic resonance imaging; RF, radio frequency.

Optimizing the production of food crops in the field requires detailed knowledge of the effects of environmental factors on the development of the plant. One of the most important processes controlling plant growth is the relation between root activity and soil functions. From this awareness, root phenomics as a means of crop development emerged. Unfortunately, many details of this relation controlling plant growth and productivity are still unknown. One of the main reasons for this is the fact that plant roots, embedded in soil, have limited observability under normal conditions. To noninvasively study root structure, in situ, during plant development, three-dimensional tomography techniques are required. Three modalities, X-ray computed tomography (CT) (Perret et al., 2007; Mooney et al., 2012), neutron CT (Matsushima et al., 2008; Tumlinson et al., 2008; Moradi et al., 2009, 2011), and magnetic resonance imaging (MRI) (Pohlmeier et al., 2008; Hillnhutter et al., 2011; Schulz et al., 2012) have been used in previous research. Neutron CT is not a commonly available technique due to the highly specialized equipment requirements and is only available in larger research facilities, while X-ray CT and MRI are readily available in most biomedical research institutions and hospitals.

X-ray CT is a very sensitive technique for studies of condensed matter, including plant roots, and can provide high-resolution images. However, its differentiation between air, water, soil, and plant material is not straightforward due to the similarity in the observed attenuation values (Tumlinson et al., 2008; Mooney et al., 2012). Not clearly defined boundaries make data segmentation and thresholding very problematic. Frequent measurements of the same root system using X-ray CT, exposing roots to the unpredictable effects of high-energy radiation, should also be avoided (Nagel et al., 2012).

Neutron CT, using cold neutrons (approximately 3–4 Å wavelength), is ideal to study organic materials that contain lots of H. Hydrogen has a large mass attenuation coefficient and thus produces excellent contrast in images. However, plants have to be grown in thin aluminum containers (slabs) using sandy soil to establish a favorable water content for experiments (Moradi et al., 2009). Recent developments in neutron radiography have made it possible to image water content in the rhizosphere using graphite columns with a diameter of 27 mm (Moradi et al., 2011). However, practical problems such as the long acquisition time per scan and the cost per experiment are somewhat prohibitive. Visibility of the roots with neutron CT is proportional to the root thickness and inversely proportional to soil moisture content.

NRC-CNRC, Aquatic and Crop Resource Development Portfolio, 435 Ellice Avenue, Winnipeg, MB, Canada R3B 1Y6. *Corresponding author (marco.gruwel@gmail.com).

Vadose Zone J.
doi:10.2136/vzj2013.08.0158
Received 30 Aug. 2013.

According to Matsushima et al. (2008), at present, cold neutron radiography is very effective for the study of thin and sparse plant materials, but MRI can be a powerful tool for the study of thick, compact plant materials (Matsushima et al., 2008). Magnetic resonance imaging is based on the observation of protons in water and would thus be a good candidate for the study of root architecture and root water content. Local water density, water mobility, and water transport can be studied with MRI. Detailed studies of plant responses to environmental impacts on the growth and branching of roots would be possible with MRI.

Magnetic resonance imaging is an extremely versatile, noninvasive technique to study water content and dynamics in many different forms of condensed matter, including plants. Static magnetic fields and the radio frequency radiation (approximately in the 10–500 MHz range) used in MRI experiments are routinely used to study or diagnose animals and humans. The many different applications of MRI in plant science from seed growth, to drought and cold stress, and to imaging of plant metabolism have recently been reviewed (Borisjuk et al., 2012). Due to its high diagnostic ability, the majority of existing MRI applications are in the biomedical field. However, plants have received substantial attention during the last decade or so, mainly due to the noninvasive nature of MRI using non-ionizing radio frequency (RF) waves (MacFall and Johnson, 1996; Borisjuk et al., 2012). In principle, MRI of plants should be simpler than imaging of humans or animals due to the lack of motion caused by breathing, pulsative cardiac motion, or involuntary abdominal motion. Magnetic resonance imaging has been used to measure three-dimensional plant structures (Köckenberger et al., 2004) with a high pixel resolution of approximately 30 μm. Dynamic processes such as water flow or diffusion in plants have also been studied with MRI (Scheenen et al., 2007). Plant seeds, too, have been subject to magnetic resonance (MR) investigations, most often to determine oil content or to study the effects of post-harvest conditions (Gruwel et al., 2002, 2008; Terskikh et al., 2005).

On the other hand, studies of plant roots using MR are not that common. The first studies focused on the ability to image roots, depending on soil conditions and an added MR contrast agent (Omasa et al., 1985; Bottomley et al., 1986; MacFall et al., 1991). Recent publications have reported the use of fast imaging techniques to reduce imaging time for the three-dimensional acquisition of root images (Haber-Pohlmeier et al., 2010) and the use of single-point imaging (SPI) in systems with low water content (Gruwel et al., 2004). When the water content becomes low and the water MR signal starts to broaden, conventional MRI fails to produce an image while SPI can still provide useful images.

The proton MRI signal is proportional to the density of water protons and modulated by spin-lattice (T_1) and spin-spin (T_2) relaxation processes. A simple system consisting of soil and roots can result in a complicated MR signal depending on the composition of the soil. Soil is an intricate mixture of hydrated particles of inorganic and organic origin, both represented by a wide size distribution and the inclusion of air pockets. Depending on the type of soil, the MR signal can suffer from a very fast decay due to a short T_2. As a result, the signal/noise ratio of the experiment will suffer significantly due to signal broadening from susceptibility artifacts caused by air bubbles, paramagnetic impurities, or the interaction of water with the porous medium (Bayer et al., 2010). However, the MR signal is still a composite of signals from water in different compartments, i.e., water in roots and soil. Using specific mixtures of soil components and plant watering intervals, the MR signal from water present in soil could significantly be reduced due to a reduction in T_2, leaving mainly the roots to be observed (Bottomley et al., 1986; MacFall and Johnson, 1996; Schulz et al., 2012). Thus segmentation of the MR signal from roots in three-dimensional MR images requires active intervention from the researcher, creating specific, controlled, in situ conditions.

Diffusion Tensor Imaging

In this study, the use of a novel MR imaging technique called diffusion tensor imaging (DTI) (Le Bihan et al., 2001; Kingsley, 2006) was investigated for the study of plant root systems and demonstrated using two different plant root architectures. Although extremely useful in medical applications (Le Bihan et al., 2001; Ciccarelli et al., 2008) tracking axons in the brain, DTI has never been applied to plant root systems or water transport in the xylem. Magnetic resonance images of the water distribution in mammalian tissues provide information on the three-dimensional density distribution of water inside these materials without any further distinction of where that water is, e.g., in a blood vessel or a nerve or just in connective tissue. To obtain information on the structure, or compartment, in which the water molecules are observed during an MR exam, T_1 or T_2 weighting is applied to manipulate the MR signal intensities from different water distributions and obtain biologically relevant contrast. This contrast is mainly used for diagnostic purposes, tracing diseases. However, structural information can indirectly be obtained when measuring water diffusion. To date, the standard MR technique to measure the effects of diffusion is the pulsed field gradient (PFG) sequence proposed by Stejskal and Tanner (1965). Standard DTI incorporates PFGs, using an echo sequence with the diffusion weighting gradients symmetrically placed around the refocusing pulse (Le Bihan et al., 2001).

In diffusion PFG MRI experiments, the diffusion constant of the water molecules is defined as the mean-square displacement in the direction of the pulsed gradients per unit time. In bulk water, diffusion in all three orthogonal directions is equally probable and thus has the same diffusion coefficient. In that case, an isotropic diffusion constant can be defined. When, due to geometric restrictions, water molecules experience different probabilities for diffusion in different directions, however, diffusion will be

anisotropic. The degree of anisotropy can be measured by applying PFGs in different directions. In general, diffusion can be described by a symmetric second-rank tensor (3 by 3 matrix), meaning that a minimum of six diffusion values will completely describe the diffusion of water in any compartment (Sen, 2004). The diffusion tensor can be characterized by three main orthogonal components (eigenvectors), with the major component describing the general direction of water movement. In many cases, the research objective is not really to study tissue diffusion per se, but rather to obtain structural or geometrical information from measured diffusion anisotropy in tissue. Mapping diffusion parameters provides information on the orientation of specific vessels, water transport pathways, or so-called fibers (e.g., axons in the brain) and the magnitude or degree of anisotropy. Performing the PFG experiments in an organized three-dimensional fashion results in a three-dimensional map of water diffusion anisotropy. Usually these maps are a collection of two-dimensional slabs stacked in the third dimension. Tractography is a three-dimensional modeling technique that uses DTI anisotropy data to visualize tracts, or pathways, for water diffusion (Wedeen et al., 2008), assuming that the direction of the largest diffusion eigenvector represents a tract or pathway. Tractography produces discrete trajectories, so called fibers or tracts, by successive stepping in the direction of the largest diffusion eigenvector, using the local voxelwise defined distributions of directions, i.e., checking for similar values in nearest neighbor voxels in the next slice. This process is known as streamline or deterministic tractography. Diffusion tensor imaging and tractography have previously been used to visualize water pathways in plants (Gruwel et al., 2013); roots have not been studied by this technique.

On the Magnetic Resonance Signal of Plant Roots and Soil

Magnetic resonance imaging of plant roots is complicated by the inhomogeneous nature of the soil–root system. Early MR studies already showed the effects of image distortion and signal loss in various types of soil (Bottomley et al., 1986). To minimize image distortions and in an effort to optimize MR relaxation parameters, sand was used as a medium for the latest MR studies (Haber-Pohlmeier et al., 2010; Stingaciu et al., 2013). The researchers used a multislice, multi-echo spin echo MR experiment. Selecting a long echo time allowed the selective observation of water with a longer T_2 (i.e., plant roots) in the case of single-echo measurements. Multi-echo experiments were used to separate the different relaxation time components of water in soil and roots.

When soil, or any other porous material, is exposed to a homogeneous magnetic field, susceptibility differences between the components (e.g., air, water, organic material, clay, etc.) cause varying internal magnetic fields (Song, 2010; Cho et al., 2012). These fields have significant effects on the relaxation of water protons in soil and roots. Initially due to direct relevance to the petroleum industry, these effects have been studied in detail over the years (Hürlimann, 1998; Sen, 2004; Mohnke and Klitzsch, 2010; Song, 2010; Cho et al., 2012). A comprehensive description relating the magnetic relaxation of water molecules in porous materials to the confining geometry, extracting the pore surface/volume ratio and tortuosity, was given by Sen (2004). Some of these theories have recently been applied to solve problems in agricultural research (Gruwel et al., 2008; Jaeger et al., 2009). However, additional problems arise when using slice-selective MR imaging techniques. Slice selection in MR is based on the assumption that in a homogeneous field, a linear gradient (here assumed in the z direction) will provide a linear spatial distribution of resonance frequencies:

$$B(\mathbf{r}) = B_0 + zG_z \quad [1]$$

where $B(\mathbf{r})$ is the magnetic field vector as a function of the coordinates ($\mathbf{r}$ represents x, y, z in a Cartesian coordinate system), B_0 is the main magnetic field, and G_z is the magnetic field gradient in the z direction. Susceptibility artifacts, depending on their strength, can destroy this condition, making spins resonate outside the selected slice (Bakker et al., 1993) and causing image distortions.

When imaging roots in soil, air pockets or bubbles will be a major cause of susceptibility artifacts. To approximate the effects of the air bubbles, we will assume the bubbles to be small and spherical. The effect of an air bubble on the local magnetic field will be the introduction of a disturbance, ΔB_z (Schenck, 1996):

$$B(\mathbf{r}) = B_0 + \Delta B_z + zG_z \quad [2]$$

For air bubbles with a radius R, the disturbance of the field near the bubble is given by

$$\Delta B_z = B_0 \frac{\Delta\chi R^3}{3r^3}\left(3\cos^2\theta - 1\right) \quad [3]$$

where $\Delta\chi$ is the difference in magnetic susceptibility (r, θ, φ are the polar coordinates , used instead of the Cartesian coordinates x, y, z). Combining the effects of the linear gradient and the susceptibility effect in Eq. [2], we obtain:

$$z - z_{\text{eff}} = \Delta z = \frac{\Delta B_z}{G_z} = \frac{B_0 \Delta\chi R^3}{G_z r^3}\left(3\cos^2\theta - 1\right) \quad [4]$$

where z_{eff} is defined by combining the last two terms in Eq. [2] as $\Delta B_z + zG_z = z_{\text{eff}}G_z$. Equation [4] clearly shows that the shape of the bubble will be distorted rather than just shifted as $\Delta z = f(r,\theta)$, and the effects are worse at higher field strength. The Hamiltonian describing the interaction of the protons with the field thus effectively becomes

$$H_z = \hbar\omega_0\left[1-\frac{4\pi}{3}\frac{R^3}{r^3}\Delta\chi\left(3\cos^2\theta-1\right)\right]I_z \quad [5]$$

where $\hbar$ is the reduced Planck's constant (Planck's constant divided by 2π), ω_0 is the proton Larmor frequency, and I_z is the proton spin angular momentum component parallel to the main magnetic field.

When the observed spins are static, a spin echo MR sequence could minimize the effects of susceptibility on the image, even though the effects will be present during frequency encoding at the time of data acquisition. For mobile spins (diffusion), susceptibility effects will significantly attenuate the observed magnetization, however, notably complicating the interpretation of relaxation rates (Grunewald and Knight, 2011).

Standard DTI acquisitions use a spin echo (two-pulse sequence) preparation. The echo time is used for diffusion weighting, placing diffusion-weighting gradients symmetrically around the refocusing pulse. During the diffusion-weighting period, the magnetization is exposed to the effects of susceptibility differences, reducing the signal intensity due to enhanced relaxation. To apply significant diffusion weighting for DTI and reduce the effects of enhanced relaxation due to susceptibility variations, a stimulated echo (three-pulse sequence) preparation should be used. The stimulated echo sequence stores the magnetization along the static field B_0, where it is not subject to perturbing interactions, during the diffusion-weighting period. As a consequence, the diffusion-weighting time can be expanded while keeping the echo time short (Merboldt et al., 1985; Cho et al., 2012). The initial drawback of a reduced MR signal intensity due to signal dissipation (factor of ½) after the second pulse is offset by the significantly expanded diffusion-weighting time, which makes this sequence very attractive for DTI experiments of plant roots. Longer diffusion-weighting times are related to a more accurate determination of water diffusion parameters (e.g., fractional anisotropy) in DTI experiments and facilitate better tractography (Rane et al., 2010).

Materials and Methods

Forage pea and field corn seeds were germinated on petri dishes and transferred to 50-mL Falcon tubes (Fisher Scientific) as soon as roots and shoots were visible. The Falcon tubes had the bottom removed and replaced with hemasorb compresses (Ardes Medical) to facilitate water uptake from the bottom (see Fig. 1) while the tubes were placed in large beakers. Plants were grown on Premier Nature Mix organic soil (Premier Tech Home and Garden). Most of the larger particles present in the soil (e.g., stones and small sticks) were removed by hand. When not being used for MR experiments, the plants were kept in a biosafety cabinet (Labconco). As reported by early MR experiments (Bottomley et al., 1986), the type of soil used for the MR experiments can have a significant influence on the quality of the acquired data. To reduce air pockets in the Falcon tubes, we performed tests with different mixtures

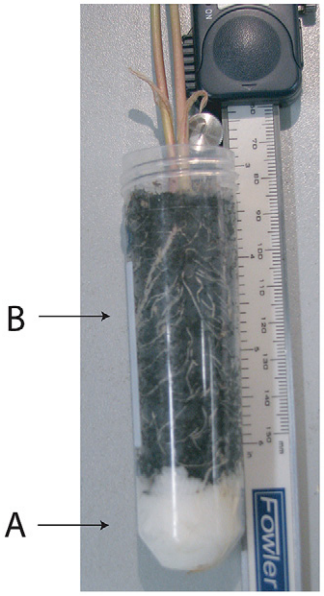

Fig. 1. Falcon tube (50 mL) with bottom removed as used in the magnetic resonance experiments, showing the hemasorp plug at the open bottom of the falcon tube to facilitate hydration (A) and the compartment containing soil and plant roots (B). In this example, two field corn kernels were grown to show root growth at the surface of the tube.

of potting soil and sand. The sand used, however, caused severe signal broadening and shifting and was thus not mixed with the potting soil. The MR experiments were performed on plants grown in potting soil only.

All micro-imaging MR experiments were performed on an Avance DRX Bruker console using a 72-mm self-shielded gradient system SGRAD 123/72/S (o.d./i.d.) (Magnex) installed in a vertical bore, 11.7-T magnet (Magnex). Experiments were performed using a home-built quadrature 4.8-cm-long by 3.5-cm i.d. bird-cage RF coil. Gradient-echo and spin-echo experiments were performed to acquire scout and anatomical reference images. Multislice spin-echo images were acquired with repetition time (TR) = 4 s, echo time (TE) = 14 ms, number of averages (NA) = 2, field of view (FOV) = 32 by 32 mm using a data matrix of 352 by 352 data points (resolution 91 by 91 μm), 36 axial slices each with a 1-mm slice thickness, and totaling 47 min of acquisition time. Spin-spin relaxation measurements of soil samples were performed using a multi-echo spin-echo sequence with 12 echoes (TE = 12–146 ms), TR = 3 s, NA = 8, and a total acquisition time of 2 h and 20 min. A modified diffusion-weighted stimulated-echo sequence, using a b value of 1000 s mm^{-2} with 10 gradient directions (Jones et al., 1999), was used for the acquisition of the DTI data (see Fig. 2). The DTI parameters used were TR = 17 s, TE = 20 ms, NA = 12, and FOV = 32 by 32 by 34 mm (34 slices of 1-mm thickness, no gap) using an in-plane data matrix of 64 by 32 points (zero filled to 64 by 64 points during image processing, resolution of 0.50 by 0.50 by 1.0 mm), totaling 20 h of acquisition time. Diffusion weighting was performed for 40 ms (Δ) with pulsed field gradients of 5-ms

(δ) duration (see Fig. 2). Diffusion tensor images were obtained from 4- to 5-d-old forage pea seedlings and 5- and 10-d-old field corn seedlings. All MRI experiments were performed at a room temperature of 20.5 ± 0.5°C.

Tractography was performed using the freely available software DSI Studio (http://dsi-studio.labsolver.org), developed by Fang Cheng Yeh at Carnegie Mellon University.

Results and Discussion

The effect of susceptibility on the MR image and spin-spin (T_2) relaxation time was briefly studied on tubes containing hydrated soil only. Multi-echo (12–146-ms) spin-echo experiments of six 2-mm-thick axial slices (perpendicular to the long axis of the tube) showed a multicomponent proton relaxation. The experiments were characterized by an initial fast decay during the first 20 to 30 ms, followed by a slower decay of the magnetization characterized by a relaxation time of T_2 = 16.7 ± 1.7 ms (n = 6). After 146 ms, a small but nonzero plateau was reached, indicating a small component to the relaxation with a rather large relaxation time. The relaxation times were calculated for selected regions of interest in the images, avoiding obvious areas containing small stones, etc. Interpretation of these relaxation times was beyond the scope of this study; however, it is clear that the relaxation of magnetization was fast and multiexponential. This multiexponentiality of the relaxation was probably caused by a combination of mechanisms, such as molecular diffusion, surface relaxation, and susceptibility effects (Sen, 2004; Jaeger et al., 2009; Grunewald and Knight, 2011; Cho et al., 2012). It should be pointed out that the contribution to the relaxation by susceptibility differences is a linear function of the field strength, $1/T_2 \approx \gamma B_0 \Delta\chi$, and thus should be significant at 11.7 T.

A representative slice of a soil MR image is shown in Fig. 3A. The circles in the figure were added as a guide to the eye. Falcon tubes have a variable diameter, being slightly narrower near the bottom of the tube. The figure shows the presence of magnetization shifted beyond the tube boundary due to susceptibility artifacts, as indicated by the arrows. In Fig. 3B a spin-echo image of a forage pea, embedded in soil, is shown on the left-hand side. The right-hand side shows a diagram explaining the orientation of the seed and shoot in the Falcon tube with respect to gravity (**g**) and the main magnetic field ($\mathbf{B_0}$). The pea, with its shoot shown in an axial slice, is marked, as well as some small sticks of organic nature (present in the soil) that hydrated well and therefore showed up in the MR image. The observed susceptibility artifacts in Fig. 3 for moderate echo times (14–20 ms) indicate that the use of a spin-echo DTI experiment would significantly suffer from destructive signal amplitude modulation during diffusion weighting.

Diffusion tensor imaging experiments require a diffusion-weighting period to be introduced during which magnetization evolves

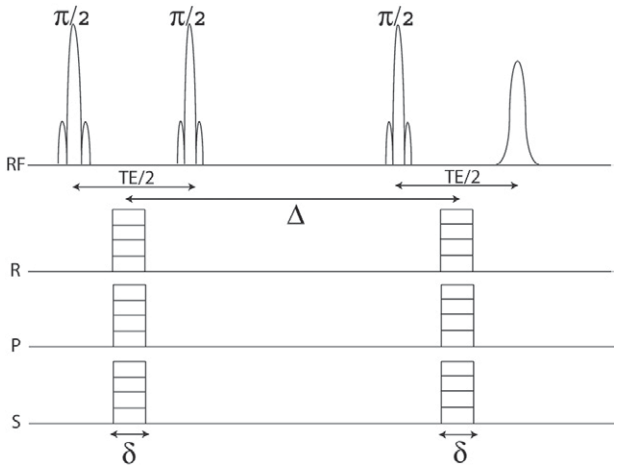

Fig. 2. Stimulated echo magnetic resonance sequence used for the diffusion tensor imaging experiments. The top line (RF) shows the three radio frequency pulses, echo timing (TE), and formation. The read, phase, and slice (R,P, and S, respectively) gradients show the timing of the pulsed diffusion gradients with a duration of δ and a separation of Δ ms. Note that other gradients, needed for the actual slice selective experiment, have been excluded for simplicity.

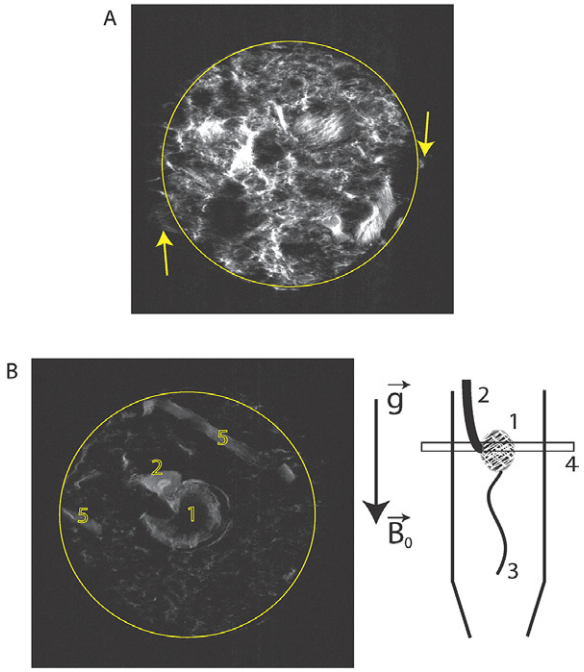

Fig. 3. Typical spin-echo experiments of (A) a soil sample, with susceptibility artifacts as indicated by the arrows, and (B,C) a growing pea: 1, pea seed; 2, pea shoot; 3, root (not visible in image slice); 4, position in the diagram of the image slice; and 5, small pieces of debris present in the soil. The diagram shows the position of the pea in the Falcon tube and the orientation with respect to the main magnetic field (B_0) and gravity (g), indicated by the arrow. The in-plane image resolution is 91 by 91 μm and the acquisition time of the data set was 47 min.

in the presence of a field gradient. In standard spin-echo DTI experiments, the magnetization will evolve in a plane perpendicular to B_0 before echo formation and signal acquisition. While being exposed to the field gradient, the magnetization will also be

affected by time evolution due to susceptibility effects introduced by the Hamiltonian of Eq. [5]. Depending on the details of this susceptibility interaction (e.g., strength and orientation), the magnetization will reduce due to additional T_2 relaxation. However, using a stimulated echo MR pulse sequence (see Fig. 2), relaxation caused by susceptibility effects can be minimized, storing the magnetization parallel to B_0 while diffusion of water molecules can proceed during a prolonged time period (Δ), selected at 40 ms for the experiments reported here.

After 2 d of germination on a petri dish, a pea showing the start of root and shoot growth was transplanted to a Falcon tube for growth in soil. Figure 4 shows DTI images of a pea obtained using the pulse sequence shown in Fig. 2. The images were obtained after 4 to 5 d of growth in soil. The black plane indicates a reference surface perpendicular to the long axis of the Falcon tube (see Fig. 3B). To facilitate the three-dimensional nature of the DTI images, a special color coding scheme was used to obtain a sense of directional preference with respect to B_0, which is parallel to the long axis of the Falcon tube. The superior to inferior direction is indicated by blue (parallel to B_0), while the left to right direction is marked by red and the posterior to anterior direction by green. Two different orientations of the same pea are shown in Fig. 4A and 4B. Both root and shoot (indicated by 1 and 2, respectively) can clearly be observed, while some of the hydrated pea is also visible (indicated by 3). Root growth parallel to the reference plane has started and can be seen in Fig. 4A, just below the pea, colored red to indicate left–right orientation.

In Fig. 5, DTI images of two field corn seedlings are shown. The images in Fig. 5A and 5B were obtained after 10 d of growth, while the images shown in Fig. 5C and 5D were obtained on a different, younger seedling (5 d of growth). Roots, shoots, and kernels can be identified in the images. Hydrated organic materials, such as small sticks, can also be seen in Fig. 5A and 5B. For convenience, some of this debris has been marked by arrows. The large root on the left-hand side of Fig. 5A and 5B does not appear to be attached to the kernel due to the FOV limitation imposed by the limited size of the RF coil.

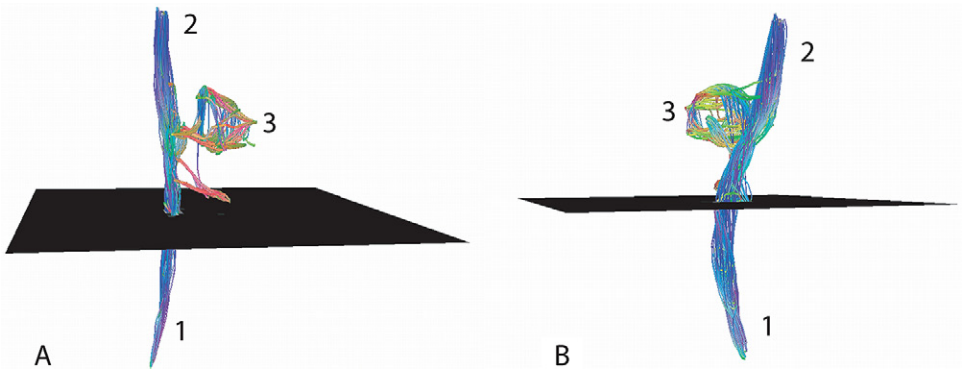

Fig. 4. Diffusion tensor imaging magnetic resonance images of a 4- to 5-d-old pea seedling, shown from two different angles. The black plane is perpendicular to the long axis of the Falcon tube and to the main magnetic field B_0. Root, shoot, and kernel are labeled as 1, 2, and 3, respectively. The black plane indicates a reference surface perpendicular to the long axis of the Falcon tube. The superior to inferior direction is indicated by blue (parallel to the main magnetic field), while the left to right direction is marked by red and the posterior to anterior direction by green. The color coding is used to provide a three-dimensional character to the two-dimensional figure. Data were acquired in 20 h with an image resolution of 0.50 by 0.50 by 1.0 mm.

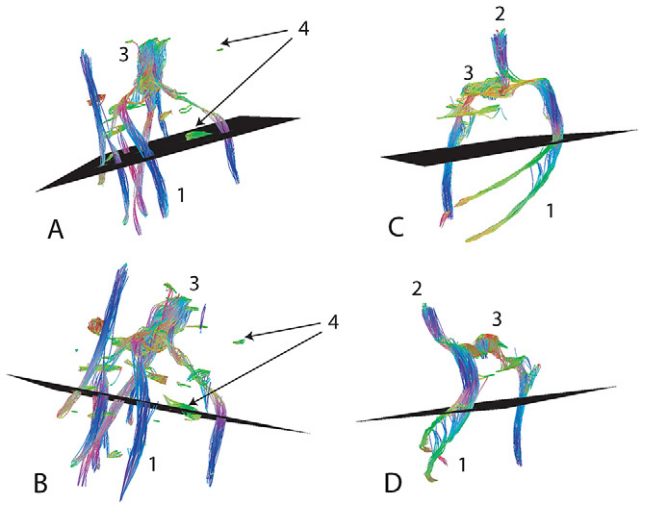

Fig. 5. Diffusion tensor imaging magnetic resonance images of corn seedlings: (A,B) a 10-d-old seedling at two different orientations, and (C,D) a 5-d-old seedling (1, root; 2, shoot; 3, kernel; 4, debris). The black plane indicates a reference surface perpendicular to the long axis of the Falcon tube. The superior to inferior direction is indicated by blue (parallel to the main magnetic field), while the left to right direction is marked by red and the posterior to anterior direction by green. The color coding is used to provide a three-dimensional character to the two-dimensional figure. Image resolution is 0.50 by 0.50 by 1.0 mm.

The processed DTI images shown in Fig. 4 and 5 were obtained using DSI Studio, neuroscience software specifically designed to perform tractography on biomedical subjects. While the goal in neuroscience is the visualization of bundles (tracts) of axons, the application of DTI and tractography in plant science, and in particular the study of roots in this study, is the visualization of root anatomy in situ. At present, the DSI Studio tractography software does not allow the delineation of root anatomy directly; however, the information to construct root anatomy is, in principle, available in the data set.

It should be noted that the spin-echo image in Fig. 3A clearly shows a more or less uniform water distribution inside the tube containing hydrated soil. Using the DTI pulse sequence, incorporating diffusion-weighting gradients in at least six or more different

orientations, only signals for water molecules with more or less restricted mobility will be observed. As a result, the background signal of freely movable water will be filtered out and Fig. 4 and 5 display only signals from water molecules that can be characterized by a high translational anisotropy. This is water restricted to movement inside roots, shoots, and other vasculature present in the seed.

Figure 5 shows that irregularities present in the soil can show up in DTI experiments as root-like structures. Most of these irregularities can be removed before the experiment by special soil preparation using mechanical filters. However, small pieces of organic debris can also be filtered out using selection procedures available in tractography. For instance, DSI Studio allows the selection of a minimum fiber length. Because most roots will uniformly grow to long lengths, small debris can be filtered out of the DTI images. Note that the soil used in this study was not mechanically filtered; instead, a quick inspection by eye was used.

All DTI images were obtained using a stimulated echo MR sequence (Merboldt et al., 1985) with a standard readout of the frequency encoded signal for each phase encoding step, repeated for each slice. As a result, the duration of the experiment was long. Typical clinical DTI experiments on the human brain, on the other hand, require only approximately 15 min of acquisition time. These experiments also acquire many slices; however, the signal is acquired using a single-shot echo planar imaging readout, which significantly increases the speed of data acquisition. A suitable variant of this technique that could possibly be implemented for future DTI experiments on roots is the propeller readout (Wang et al., 2005), minimizing the total acquisition time. Further acceleration of signal acquisition can be accomplished using parallel imaging using phased-array RF coils (Larkman and Nunes, 2007). For use in plant sciences only, the medical tractography software used here could be adapted to visualize whole roots. In particular, the software can be adapted to show whole roots instead of fiber bundles.

The DTI experiments on plant roots shown here are of relatively low resolution (0.50 by 0.50 by 1.0 mm); however, these images are three-dimensional representations of root architecture and are hard to obtain using other techniques. Recent developments in high-throughput plant phenotyping, using visible light photography in a two-dimensional (thin slab) rhizotron (Nagel et al., 2012), resulted in images with a 0.230-mm pixel (in plane) resolution. Semi-three-dimensional images of plant roots, consisting of a two-dimensional surface projection onto the (special material) plant pot, were obtained with near-infrared techniques (Dixit, 2013). Neither of these developments introduced a true three-dimensional imaging technique. Magnetic resonance diffusion tensor imaging is able to obtain three-dimensional images of plant roots, and the technique needs to be optimized to be used in future high-throughput experiments. Low-field (0.4T) MRI systems would be extremely useful for this purpose. These low-field systems consist of a four-post, open-concept magnet with enough clearance for whole potted plants and allow the incorporation of a conveyor belt system as part of a root phenotyping program. Additionally, the use of a low magnetic field would automatically reduce possible susceptibility artifacts.

In conclusion, we have shown that plant roots can be imaged, in situ, using DTI, a magnetic resonance application. To minimize susceptibility artifacts, a stimulated echo MR sequence was used, allowing significant diffusion weighting while minimizing MR signal loss. Further development of the DTI pulse sequence and incorporation of fast readout scans will strongly reduce the total acquisition time and make high-resolution imaging possible in acceptable time frames.

Acknowledgments

I would like to thank Dr. Sue Abrams (University of Saskatchewan, Structural Sciences Centre) for her continued interest and encouragement, and Doug Durnin (University of Manitoba, Department of Plant Science) for his help with the experiments.

References

Bakker, C., R. Bhagwandien, M. Moerland, and M. Fuderer. 1993. Susceptibility artifacts in 2DFT spin-echo and gradient-echo imaging: The cylinder model revisited. Magn. Reson. Imaging 11:539–548. doi:10.1016/0730-725X(93)90473-Q

Bayer, J.V., F. Jaeger, and G.E. Schaumann. 2010. Proton nuclear magnetic resonance (NMR) relaxometry in soil science applications. Open Magn. Reson. J. 3:15–26.

Borisjuk, L., H. Rolletschek, and T. Neuberger. 2012. Surveying the plant's world by magnetic resonance imaging. Plant J. 70:129–146. doi:10.1111/j.1365-313X.2012.04927.x

Bottomley, P.A., H.H. Rogers, and T.H. Foster. 1986. NMR imaging shows water distribution and transport in plant root systems in situ. Proc. Natl. Acad. Sci. 83:87–89. doi:10.1073/pnas.83.1.87

Cho, H.J., E.E. Sigmund, and Y. Song. 2012. Magnetic resonance characterization of porous media using diffusion through internal magnetic fields. Materials 5:590–616. doi:10.3390/ma5040590

Ciccarelli, O., M. Catani, H. Johansen-Berg, C. Clark, and A. Thompson. 2008. Diffusion-based tractography in neurological disorders: Concepts, applications, and future developments. Lancet Neurol. 7:715–727. doi:10.1016/S1474-4422(08)70163-7

Dixit, S. 2013. Translation of digital phenotypic traits: From image to commercial relevance. Paper presented at: Plant and Animal Genome XXI Conference, San Diego. 12–16 Jan. 2013.

Grunewald, E., and R. Knight.. 2011. The effect of pore size and magnetic susceptibility on the surface NMR relaxation parameter T_2*. Near Surf. Geophys.9:169–178. doi:10.3997/1873-0604.2010062

Gruwel, M.L.H., P.K. Ghosh, P. Latta, and D.S. Jayas. 2008. On the diffusion constant of water in wheat. J. Agric. Food Chem. 56:59–62. doi:10.1021/jf0720537

Gruwel, M.L.H., P. Latta, U. Sboto-Frankenstein, and P. Gervai. 2013. Visualization of water transport pathways in plants using diffusion tensor imaging. Prog. Electromagn. Res. C 35:73–82. doi:10.2528/PIERC12110506

Gruwel, M.L.H., P. Latta, V. Volotovskyy, M. Šramek, and B. Tomanek. 2004. Magnetic resonance imaging of seeds by use of single point acquisition. J. Agric. Food Chem. 52:4979–4983. doi:10.1021/jf049078f

Gruwel, M.L.H., X.S. Yin, M.J. Edney, S.W. Schroeder, A.W. MacGregor, and S. Abrams. 2002. Barley viability during storage: Use of magnetic resonance as a potential tool to study viability loss. J. Agric. Food Chem. 50:667–676. doi:10.1021/jf0108617

Haber-Pohlmeier, S., M. Bechtold, S. Stapf, and A. Pohlmeier. 2010. Water flow monitored by tracer transport in natural porous media using magnetic resonance imaging. Vadose Zone J. 9:835–845. doi:10.2136/vzj2009.0177

Hillnhutter, C., R.A. Sikora, E.-C. Oerke, and D. van Dusschoten. 2011. Nuclear magnetic resonance: A tool for imaging belowground damage caused by *Heterodera schachtii* and *Rhizoctonia solani* on sugar beet. J. Exp. Bot. 63:319–327. doi:10.1093/jxb/err273

Hürlimann, M.D. 1998. Effective gradients in porous media due to susceptibility differences. J. Magn. Reson. 131:232–240. doi:10.1006/jmre.1998.1364

Jaeger, F., S. Bowe, H. Van As, and G. Schaumann. 2009. Evaluation of ^{1}H NMR relaxometry for the assessment of pore-size distribution in soil samples. Eur. J. Soil Sci. 60:1052–1064. doi:10.1111/j.1365-2389.2009.01192.x

Jones, D., M. Horsfield, and A. Simmons. 1999. Optimal strategies for measuring diffusion in anisotropic systems by magnetic resonance imaging. Magn. Reson. Med. 42:515–525.

Kingsley, P.B. 2006. Introduction to diffusion tensor imaging mathematics: II. Anisotropy, diffusion-weighting factors, and gradient encoding schemes. Concepts Magn. Reson. A 28:123–154. doi:10.1002/cmr.a.20049

Köckenberger, W., C. De Panfilis, D. Santoro, P. Dahiya, and S. Rawsthorne. 2004. High resolution NMR microscopy of plants and fungi. J. Microsc. 214:182–189. doi:10.1111/j.0022-2720.2004.01351.x

Larkman, D.J., and R.G. Nunes. 2007. Parallel magnetic resonance imaging. Phys. Med. Biol. 52(7):R15. doi:10.1088/0031-9155/52/7/R01

Le Bihan, D., J.-F. Mangin, C. Poupon, C.A. Clark, S. Pappata, N. Molko, and H. Chabriat. 2001. Diffusion tensor imaging: Concepts and applications. J. Magn. Reson. Imaging 13:534–546. doi:10.1002/jmri.1076

MacFall, J.S., and G.A. Johnson. 1996. Plants, seeds, roots, and soils as applications of magnetic resonance microscopy. In: eMagRes. John Wiley & Sons, New York. doi:10.1002/9780470034590.emrstm0396.pub2

MacFall, J., G. Johnson, and P. Kramer. 1991. Comparative water uptake by roots of different ages in seedlings of loblolly pine (*Pinus taeda* L.). New Phytol. 119:551–560. doi:10.1111/j.1469-8137.1991.tb01047.x

Matsushima, U., N. Kardjilov, A. Hilger, W. Graf, and W. Herppich. 2008. Application potential of cold neutron radiography in plant science research. J. Appl. Bot. Food Qual. 82:90–98.

Merboldt, K.-D., W. Hanicke, and J. Frahm. 1985. Self-diffusion NMR imaging using stimulated echoes. J. Magn. Reson. 64:479–486. doi:10.1016/0022-2364(85)90111-8

Mohnke, O., and N. Klitzsch. 2010. Microscale simulations of NMR relaxation in porous media considering internal field gradients. Vadose Zone J. 9:846–847. doi:10.2136/vzj2009.0161

Mooney, S., T. Pridmore, J. Helliwell, and M. Bennett. 2012. Developing x-ray computed tomography to non-invasively image 3-D root systems architecture in soil. Plant Soil 352:1–22. doi:10.1007/s11104-011-1039-9

Moradi, A.B., A. Carminati, D. Vetterlein, P. Vontobel, E. Lehmann, U. Weller, et al. 2011. Three-dimensional visualization and quantification of water content in the rhizosphere. New Phytol. 192:653–663. doi:10.1111/j.1469-8137.2011.03826.x

Moradi, A.B., H.M. Conesa, B. Robinson, E. Lehmann, G. Kuehne, A. Kaestner, et al. 2009. Neutron radiography as a tool for revealing root development in soil: Capabilities and limitations. Plant Soil 318:243–255. doi:10.1007/s11104-008-9834-7

Nagel, K.A., A. Putz, F. Gilmer, K. Heinz, A. Fischbach, J. Pfeifer, et al. 2012. GROWSCREEN-Rhizo is a novel phenotyping robot enabling simultaneous measurements of root and shoot growth for plants grown in soil-filled rhizotrons. Funct. Plant Biol. 39:891–904.

Omasa, K., M. Onoe, and H. Yamada. 1985. NMR imaging for measuring root system and soil water content. Environ. Control Biol. 23:99–102.

Perret, J., M. Al-Belushi, and M. Deadman. 2007. Non-destructive visualization and quantification of roots using computed tomography. Soil Biol. Biochem. 39:391–399. doi:10.1016/j.soilbio.2006.07.018

Pohlmeier, A., A. Oros-Peusquens, M. Javaux, M. Menzel, J. Vanderborght, J. Kaffanke, et al. 2008. Changes in soil water content resulting from root uptake monitored by magnetic resonance imaging. Vadose Zone J. 7:1010–1017. doi:10.2136/vzj2007.0110

Rane, S., G. Nair, and T.Q. Duong. 2010. DTI at long diffusion time improves fiber tracking. NMR Biomed. 23:459–465. doi:10.1002/nbm.1482

Scheenen, T.W.J., F.J. Vergeldt, A.M. Heemskerk, and H. Van As. 2007. Intact plant magnetic resonance imaging to study dynamics in long-distance sap flow and flow-conducting surface area. Plant Physiol. 144:1157–1165. doi:10.1104/pp.106.089250

Schenck, J.F. 1996. The role of magnetic susceptibility in magnetic resonance imaging: MRI magnetic compatibility of the first and second kinds. Med. Phys. 23:815. doi:10.1118/1.597854

Schulz, H., J.A. Postma, D. van Dusschoten, H. Scharr, and S. Behnke. 2012. 3D reconstruction of plant roots from MRI images. In: G. Csurka and J. Braz, editors, Proceedings of the International Conference on Computer Vision Theory and Applications (VISAPP), Rome. 24–26 Feb. 2012. SciTePress. p. 24–33.

Sen, P.N. 2004. Time-dependent diffusion coefficient as a probe of geometry. Concepts Magn. Reson. A 23:1–21. doi:10.1002/cmr.a.20017

Song, Y.-Q. 2010. Recent progress of nuclear magnetic resonance applications in sandstones and carbonate rocks. Vadose Zone J. 9:828–834. doi:10.2136/vzj2009.0171

Stejskal, E., and J. Tanner. 1965. Spin diffusion measurements: Spin echoes in the presence of a time-dependent field gradient. J. Chem. Phys. 42:288. doi:10.1063/1.1695690

Stingaciu, L., H. Schulz, A. Pohlmeier, S. Behnke, H. Zilken, M. Javaux, and H. Vereecken. 2013. In situ root system architecture extraction from magnetic resonance imaging for water uptake modeling. Vadose Zone J. 12(1). doi:10.2136/vzj2012.0019

Terskikh, V.V., J.A. Feurtado, C. Ren, S.R. Abrams, and A.R. Kermode. 2005. Water uptake and oil distribution during imbibition of seeds of western white pine (*Pinus monticola* Dougl. ex D. Don) monitored in vivo using magnetic resonance imaging. Planta 221:17–27. doi:10.1007/s00425-004-1426-z

Tumlinson, L.G., H. Liu, W.K. Silk, and J.W. Hopmans. 2008. Thermal neutron computed tomography of soil water and plant roots. Soil Sci. Soc. Am. J. 72:1234–1242. doi:10.2136/sssaj2007.0302

Wang, F.-N., T.-Y. Huang, F.-H. Lin, T.-C. Chuang, N.-K. Chen, H.-W. Chung, et al. 2005. PROPELLER EPI: An MRI technique suitable for diffusion tensor imaging at high field strength with reduced geometric distortions. Magn. Reson. Med. 54:1232–1240. doi:10.1002/mrm.20677

Wedeen, V.J., R.P. Wang, J.D. Schmahmann, T. Benner, W.Y.I. Tseng, G. Dai, et al. 2008. Diffusion spectrum magnetic resonance imaging (DSI) tractography of crossing fibers. Neuroimage 41:1267–1277. doi:10.1016/j.neuroimage.2008.03.036